PRODUCTION OF *n*-PROPYL ACETATE BY REACTIVE DISTILLATION
Experimental and Theoretical Study

M. Brehelin[1], F. Forner[2], D. Rouzineau[1], J.-U. Repke[2], X. Meyer[1], M. Meyer[1]* and G. Wozny[2]

[1]**Laboratoire de Génie Chimique, INP ENSIACET, Toulouse, France.**
[2]**Institute of Process and Plant Technology, Technische Universität Berlin, Germany.**

Abstract: First steps of the development of a catalytic reactive distillation process for the production of *n*-propyl acetate based on experiments and simulations are proposed. The kinetics for homogeneously (sulphuric acid) and heterogeneously (Amberlyst 15) catalysed reaction were investigated and the constants for a pseudo-homogeneous model are presented. Pilot plant experiments were performed using a homogeneous strong acid catalyst in a packed column. A top-column decanter is used to withdraw the aqueous phase and to reflux the organic phase. Simulation results are in good agreement with experimental data. Thermodynamics non-idealities are taken into account using VLE and LLE NRTL interaction parameters. Alcohol conversion and *n*-propyl acetate purity may be dramatically increased just by adding to the pilot plant a stripping section in an additional column: six different configurations are identified to achieve such a production. The startup is studied in order to determine the best strategy to achieve steady-state conditions. The strong influence of the composition of the initial charging in the decanter can be seen and an initial charging of the two-phase top product leads to the fastest startup.

Keywords: reactive distillation; kinetics; startup; experimental data; *n*-propyl acetate.

**Correspondence to:*
Dr M. Meyer, Laboratoire de Génie Chimique, INP ENSIACET, Toulouse, France.
E-mail: michel.meyer@ensiacet.fr

INTRODUCTION

The combination of reaction and distillation in one reactive distillation (RD) unit can lead to significant reduction of investment and operational cost. However, interactions between reactions and separation increase complexity and require a better understanding of the process. Whereas RD is intensively studied for years, only few works have been published on vapour–liquid–liquid (VLL) systems, thus our investigations focus on VLL reactive systems.

Experimental investigations have already been published for the production of butyl acetate (Steinigeweg and Gmehling, 2002) or amyl acetate (Chiang *et al.*, 2002) but, to the best of our knowledge, none for *n*-propyl acetate reactive distillation; thus, information about *n*-propyl acetate synthesis can hardly be found in literature. Investigations on reactive membrane separation have led Huang *et al.* (2005) to publish data on chemical equilibrium. Bart *et al.* (1996) have published a kinetic modelling of the *n*-propyl acetate synthesis catalysed by an ion exchange resin (Dowex) as well as Steinigeweg (2003) with the Amberlyst-15. Unfortunately, uncertainty remains on the chemical equilibrium constant value. Finally, no data about reactive distillation pilot-plant experiments is published.

However, reactive distillation column design requires reliable kinetic data in addition to other crucial information such as phase equilibria. Methods carried out to assess the reactive distillation process feasibility are often based on residue curve maps (RCM) for non-reactive distillation, and on reactive residue curve maps (rRCM) for reactive distillation. In addition to the four pure components, three azeotropes are the singular points of the *n*-propyl acetate synthesis reaction rRCM (Table 1). Two of these azeotropes (PrOH/PrOAc and PrOH/H_2O) are remaining from the non-reactive RCM although two others involving reactive species (PrOAc/H2O and PrOH/PrOAc/H_2O which are both heterogeneous) disappear; the last singular point of this rRCM is a quaternary reactive azeotrope. The chemical equilibrium constant value has a great influence on the liquid phase stability of this point (but not on its topological stability since it is always an unstable node): when a value of 20 (Huang *et al.*, 2005) is used, the reactive azeotrope is homogeneous, although a value of 48.8 (Okasinski and Doherty, 2000) leads to a heterogeneous reactive azeotrope.

Table 1. Singular points of *n*-propyl acetate synthesis reaction rRCM.

System	*T* (°C)	Stability		Molar composition
		Topological	Physical	
HOAc	117.9	SN		
PrOAc	101.5	Sa		
H_2O	100.0	Sa		
PrOH	97.2	SN		
PrOH/PrOAc	94.7	Sa	Homogeneous	0.625/0.375
PrOH/H_2O	87.8	Sa	Homogeneous	0.432/0.568
HOAc/PrOH/PrOAc/H_2O	85.4	UN	Homogeneous	0.069/0.309/0.146/0.476
	84.0		Heterogeneous	0.059/0.245/0.262/0.435

These effects are clearly illustrated in Figure 1 for which rRCM have been computed using a previous work on the rRCM calculation taking into account rigorous VLLE equilibria (Brehelin *et al*., 2006); the transformed variable coordinates (Ung and Doherty, 1995) are used with *n*-propyl acetate as the reference component. For the sake of better representation of the chemical and phase equilibria complexity, rRCM in molar composition are represented too in Figure 1 (bottom).

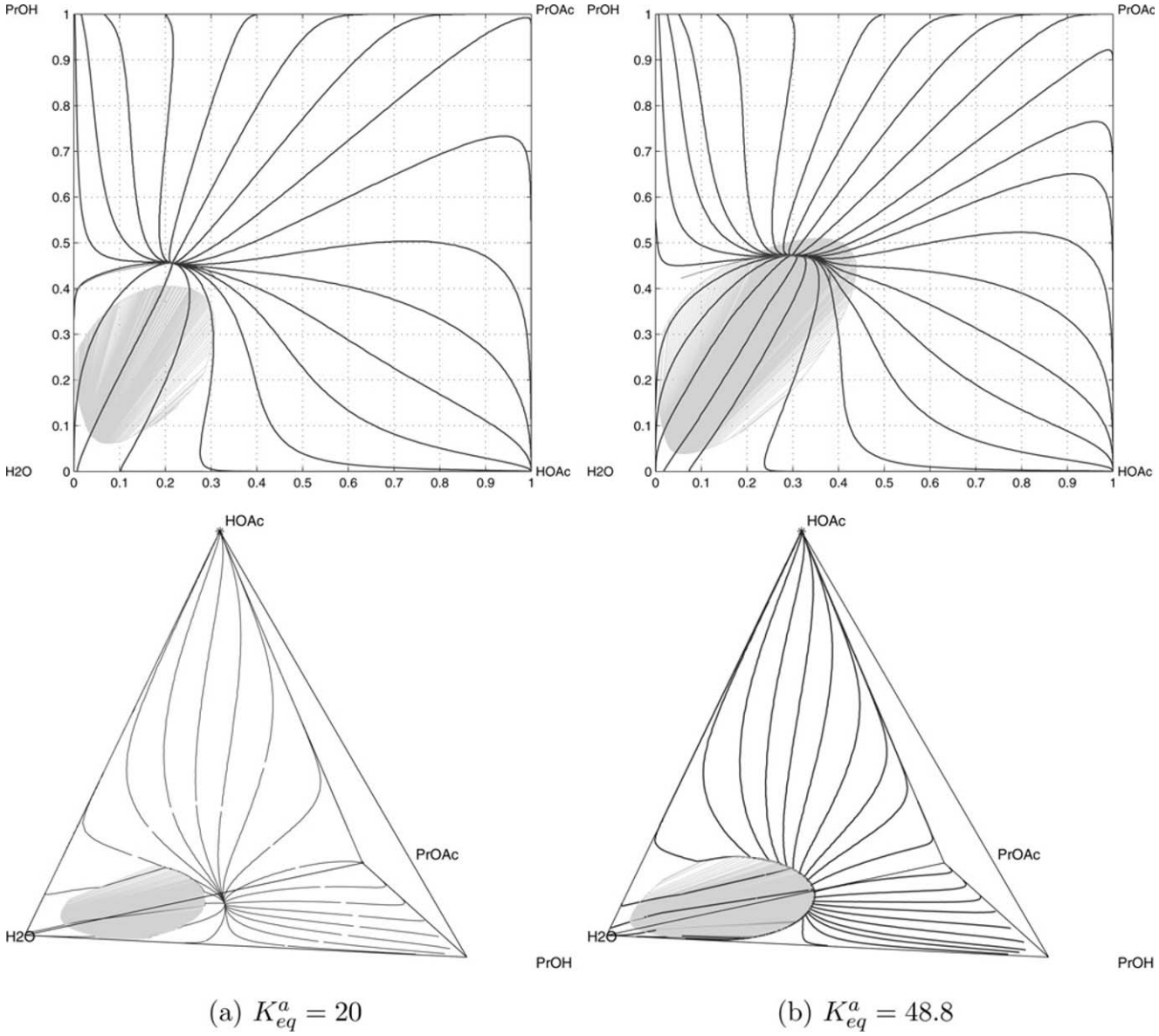

Figure 1. n-Propyl acetate synthesis reaction rRCM in transformed (top) and molar (bottom) compositions showing the miscibility gap for two values of the chemical equilibrium.

As a consequence, great attention has to be paid to the chemical and phase equilibria determination in order to perform the design of such a process. Therefore, this article presents the first steps of an approach to the development of a RD process for the production of *n*-propyl acetate: the catalysed reaction kinetics are firstly investigated in order to employ a simulation environment based on an equilibrium stage model; in parallel pilot plant experiments are carried out in order to validate this simulation tool. On the basis of these results, an optimal startup strategy is proposed and several process configurations are studied in order to propose the best setup for high purity *n*-propyl acetate production.

EXPERIMENTAL SECTION

Materials and Analysis

The chemicals used for the kinetic study were of analytical grade (rectapur); Amberlyst 15 and concentrated sulphuric acid were selected as catalysts. For the reactive distillation experiments, the chemicals were of reaction grade (99.5%) and sulphuric acid was the catalyst. All samples were analysed by gas chromatography (Varian 3800) using cross-linked polyethylene glycol CP-WAX 52 CB 30 m $\times$ 0.32 mm column with FID detector. For the homogeneously catalyzed kinetic runs, the acetic acid concentration has been determined using titration; additional titrations were performed with a METTLER DL 35 Karl–Fischer-Titrator to measure the quantity of water formed during the reaction.

A data reconciliation process was led in order to appreciably increase reliability and consistency of results: the elimination of aberrant measurements is performed on the base of the atomic conservation (Fillon *et al.*, 1995). An accuracy of molar fractions of 3% can thus be expected.

Kinetic Experiments

Kinetic experiments were conducted in a thermostated three-neck glass reactor with a volume of 500 cm^3. One neck was connected to a thermometer and another was devoted to the GC sampling; a cold trap, in addition to a reflux condenser, was installed in the third neck to avoid any loss of volatile components. The temperature of the heating jacket was kept constant within ± 0.1 K. Before each kinetic experiment was started, both reactants were brought to reaction temperature separately; when the desired temperature was reached, reactants and catalyst were added to the reactor and time measurement was started. Liquid samples of about 1 cm^3 volume, without any catalyst in case of Amberlyst 15, were taken using a syringe and cooled to 253 K to avoid any further reaction. The contents were stirred by a magnetic stirrer. The stirrer speed is fixed in such a manner that it has no influence on the reaction rate (Steinigeweg and Gmehling, 2002); thus, the external mass transfer resistance seems not to be significant (Pitochelli, 1980) and the internal mass transfer resistance was neglected on the basis of a Weisz and Hicks criterion calculation (Weisz and Hicks, 1962).

Reactive Distillation Experiments

Setup

Experiments were performed in a 4-m of glass column with an inner diameter of 80 mm (Figure 2): the reactive section is packed with 8 mm $\times$ 8 mm glass Raschig rings and the rectifying section contained Sulzer-CY packing; the liquid phase total hold-up estimated by the Engel's method (Engel *et al.*, 2001) is of 80 ml. Each reactant is fed separately in the column. Reaction was catalysed by homogeneous sulphuric acid fed at the top of the reactive section with a weight amount of 1.3% in the acetic acid flow. The reboiler, with a liquid hold-up of approximately 10 dm^3 was heated by an oil-boiler and insulated by mineral wool whereas the column was equipped with two couples of heating mantles; the maximal heating power measured was of 3 kW. Distillate was collected in a decanter operated at ambient temperature and all organic phase was refluxed at the top of the column. Feed and product flows were measured by balances. Temperatures were measured by Pt-100 thermometers installed at the bottom of each section, as well as in the feed stream, the reboiler and the condenser.

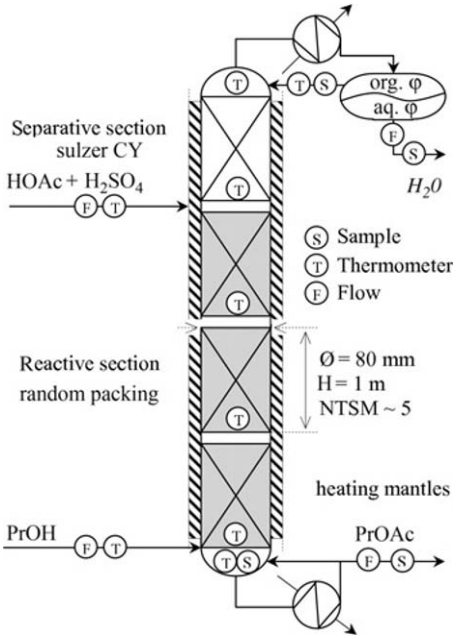

Figure 2. Conceptual schema of the pilot-plant used to perform reactive distillation experiments.

Startup

The startup strategy was to start with empty reboiler and decanter; the preheated feeds and a gradual heat duty at the reboiler led the mixture to boiling point. When a sufficient amount of distillate was collected to the decanter the reflux pump was turned-on and the set-point was adjusted in order to reflux all the organic phase.

Results

Although this pilot plant has not been built especially for the *n*-propyl acetate production by reactive distillation—its design is far from optimal since an acetic acid conversion of 79% with a molar purity of *n*-propyl acetate of 64% has been achieved—dynamic and steady-state simulation can be performed on the base of these experimental results.

Thus the aim of these runs was to obtain experimental data useful to validate our simulations. The material balances of a

Table 2. Material balances of a typical reactive distillation run.

	HOAc Feed	PrOH feed	Aqueous phase	Bottoms	I–O (%)
F (mol h^{-1})	46.63	41.00	38.57	53.50	4.9
	Molar composition				Δn (mol)
HOAc	1	0	0.018	0.173	−36.7
PrOH	0	1	0.008	0.131	−33.7
PrOAc	0	0	0.004	0.638	+34.3
H_2O	0	0	0.970	0.058	+40.6

typical reactive distillation run summarized in Table 2 show the reliability of a typical steady-state.

RESULTS AND ANALYSES

Kinetic Parameter Identification

A pseudo-homogeneous model [equation (1)] is used to describe the reaction catalysed both with Amberlyst 15 or sulphuric acid. This choice is theoretically supported by the fact that the heterogeneous catalyst swells in contact with polar solvents making the sulfonic groups of the catalyst readily accessible to reactants; in such a model, the ion-exchange resin is thought to act as solvated protons; consequently, rate constants can be expressed as a function of proton amount; its temperature dependency is expressed by Arrhenius' law [equation (2)], so that four adjustable parameters ($K_{f,o}$, $K_{a,o}$, E_f, E_a) have to be fitted (Table 3).

$$r = \frac{1}{\nu_i}\frac{dn_i}{dt} = n_{H^+}K_f\left(a_{HOAc}a_{PrOH} - \frac{a_{PrAc}a_{H_20}}{K_a}\right) \quad (1)$$

$$K_i = K_{i,0}.\exp\left(-\frac{E_i}{R{:}T}\right) \quad (2)$$

The molar fractions of acetic acid, computed by the numerical integration of the kinetic equation, are compared with the experimental ones. The activity coefficients were calculated using the NRTL equation of which interaction parameters are given in Table 4(a). Parameters are fitted by minimization of the criterion defined by equation (3) using a least square method. The mean value of this criterion, i.e., the mean relative deviation—assumed to be representing the accuracy of the model—is inferior to 5%.

$$\text{crit} = \min \sum_{\text{all samples}} (x^{\text{calc}}_{HOAc} - x^{\text{exp}}_{HOAc})^2 \quad (3)$$

The theoretical dependence on temperature of the equilibrium constant is shown in Figure 3: the obvious agreement between our chemical equilibrium data and Huang's ones [almost 20 on the range temperature (80–110°C)] reinforce the validity of our identification. Moreover experimental data

Table 3. Parameters of the kinetic model for sulphuric acid and Amberlyst 15 as catalysts.

	K_o (mol s^{-1}·mol$^{-1}_{H+}$)	E_a (J mol^{-1})
Esterification (H_2SO_4)	7.699×10^4	37,084
Esterification (A15)	2.576×10^6	51,540
Chemical equilibrium	17.52	−366

Table 4. (a) NRTL parameters for the calculation of activity coefficients and phase equilibria (Huang *et al.*, 2005; Okasinski and Doherty, 2000).

I	J	a_{ij} (cal mol^{-1})	b_{ij}(cal mol^{-1})	α
HOAc	PrOH	− 327.52	256.90	0.3044
HOAc	PrOAc	− 410.39	1050.56	0.2970
HOAc	H_2O	− 342.20	1175.72	0.2952
PrOH	PrOAc	− 340.02	111.74	0.3005
PrOH	H_2O	− 152.51	1866.34	0.3747
PrOAc	H_2O	− 667.45	3280.60	0.2564

Table 4. (b) Liquid–liquid NRTL parameters for the ternary PrOH/PrOAc/H_2O (Sørensen and Arlt, 1982).

I	J	a_{ij} (cal mol^{-1})	b_{ij}(cal mol^{-1})	α
PrOH	PrOAc	−86.17	467.23	0.2
PrOH	H_2O	−1102.18	2949.20	0.2
PrOAc	H_2O	−602.82	3023.92	0.2

are related to the standard enthalpy of reaction by the van't Hoff equation: experimental and theoretical values of the standard energy of reaction are concordant (−1.02 and −1.69 kJ mol^{-1}).

Simulation

Steady state

Steady-state simulations based on an equilibrium model were carried out using the commercial software ProSim Plus; the activity coefficients are derived from NRTL model [Table 4(a)] and used for phase equilibriums as well as for the kinetic model. It will be shown later that distillate stream is free of acetic acid so specific liquid–liquid NRTL parameters are used to compute phase equilibria into the decanter [Table 4(b)]. Vapour phase association due to the presence of acetic acid in the system has been accounted for with the chemical theory (Marek and Standard, 1954).

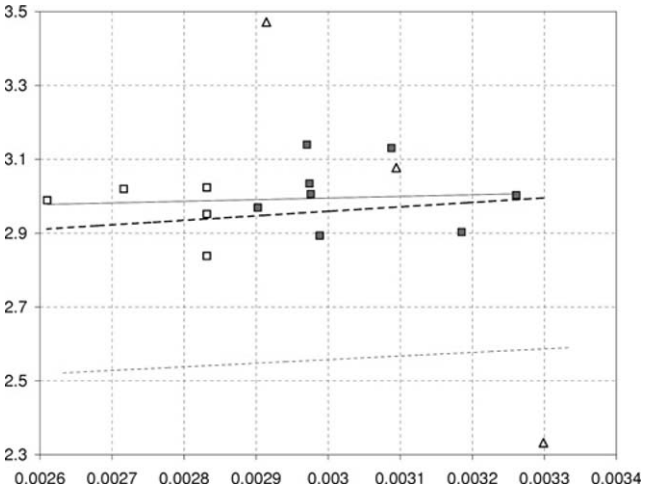

Figure 3. Natural logarithm of the equilibrium constant against reciprocal temperature. This study (■) Huang *et al.* (□), Bart *et al.* (△), Steinigeweg (···) and theoretical estimation based on enthalpy of formation (– – –).

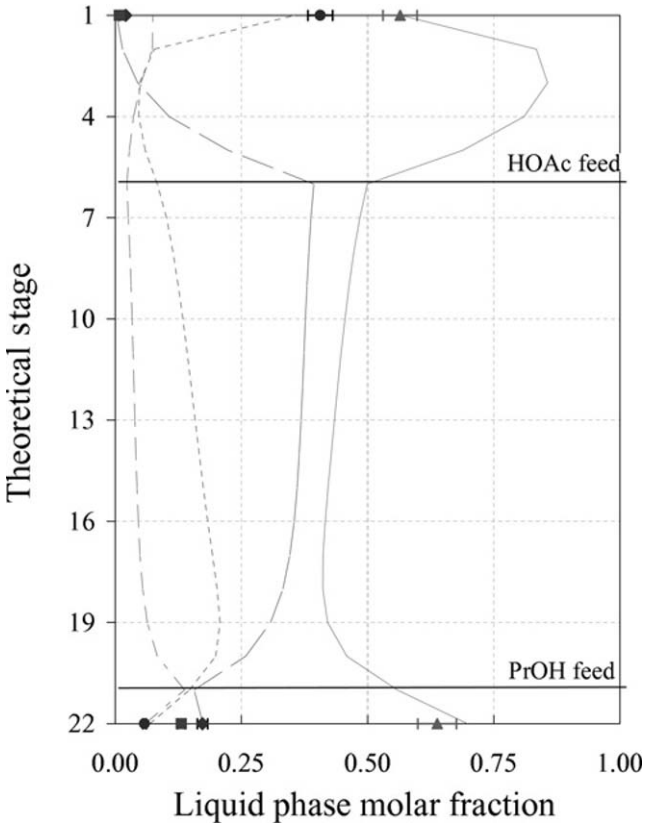

Figure 4. Liquid composition profile along theoretical stages. HOAc (▽), PrOH (□), PrOAc (△), H_2O (○).

Figure 4 illustrates the good agreement observed between experimental data and simulation (mean deviation of 3.5% on molar composition).

Startup analysis

The startup of a reactive distillation column is a very complex, time and energy consuming process. The dynamic process behaviour becomes even more complex in case of a miscibility gap at the column top which is influenced by the reaction. Special attention has to be paid to the behaviour of the decanter during startup in order to rapidly reach conditions leading to the phase split. Reepmeyer *et al.* (2004) have analysed the startup of homogeneously catalysed reactive distillation in tray columns and have shown that initial charging of product to the column trays can lead to significant reduction of startup time. Tran (2005) have studied non-reactive three phase distillation in a tray column with a decanter. They have shown both by experiment and simulation that the startup time depends strongly on the composition of the initial hold-up in the decanter. Surprisingly, for the system ethanol/water/cyclohexane, initial charging of ethanol (bottom product) to the decanter led to a reduction of about 60% of startup time. On the other hand charging with a two phase mixture close to steady state composition extended the startup time (Tran 2005).

The startup process which is considered in this contribution begins when feed is entering the initially cold and empty column. The dry packing is wetted and the column bottom is filled up until the reboiler is switched on. Vapour starts rising in the column and partly condenses on the cold internals. When it reaches the top, reflux from the condenser enters the column and finally all variables reach the steady-state values. During this process the hydraulic and thermodynamic variables underlie large changes. The hold-up in the column and the flow rates change from zero to their steady state values. The temperatures rise from ambient temperature to the boiling temperature. Due to these transitions the startup cannot be described by a standard dynamic equilibrium stage model which is only valid for conditions close to the operating point. Different sets of equations are therefore needed for the different distinguishable phases of the startup, requiring a switching between these model equations at certain points for every single stage *j* separately. This procedure eventually leads to an equilibrium stage model for the operating range consisting of the MESH equations, reaction kinetics and hydraulic correlations [pressure drop and liquid hold-up correlations from Engel *et al.* (2001) for the stages, Toricelli type correlations for the liquid hold-up in reboiler and decanter]. During the startup simulation, switching concerning liquid and vapour flow rates assures that the hydraulic correlations are only considered if a certain amount of liquid has accumulated on a stage (liquid hold-up correlation) or a certain pressure drop has built up (pressure drop correlation). The corresponding flow rates are otherwise set to zero. At low temperatures liquid and vapour are not in equilibrium, and the pressure is therefore first set to a constant initial value, the temperature is calculated independently from the VLE and the vapour phase is not considered. When during the heating-up the temperature calculated by the startup model reaches the additionally calculated bubble point temperature at this initial pressure and the current liquid composition, then the vapour phase is included in the model and temperature and pressure correspond to the VLE [switching according to equation (4)]. In the decanter model the possible appearance of a second liquid phase is considered during the whole startup by continuously checking the liquid composition.

$$\begin{aligned} &\text{If} \quad T_j \geq T_j^{LV} \text{then} \\ &\qquad T_j = T_j^{LV} \\ &\qquad V_{\text{section}} = HU_j^L v^L + HU_j^V v^V \\ &\qquad T_j \neq T_j^{LV} \\ &\text{Else} \qquad\quad p_j = \text{const.} \\ &\qquad\quad\;\; HU_j^V = 0 \end{aligned} \tag{4}$$

The developed simulation model has been validated with startup data from the presented experiment. Figure 5 shows the comparison between the concentrations in the reboiler and the organic phase in the decanter during startup. The startup begins with the start of the feeding and the reboiler duty ramp ($t = 0$). Since reboiler and decanter are initially empty, the first liquid samples are taken after 1–1.5 hs. The simulation describes the dynamic behaviour very well, including the instant formation of a miscibility gap when the first subcooled condensate enters the decanter.

In the following the startup process with different initial charging of the decanter is analysed using the validated model. During all the simulation runs the reboiler is initially empty and filled by the feeds entering the column. When the level is high enough the reboiler duty is increased stepwise to the steady-state value. In case of an initially charged

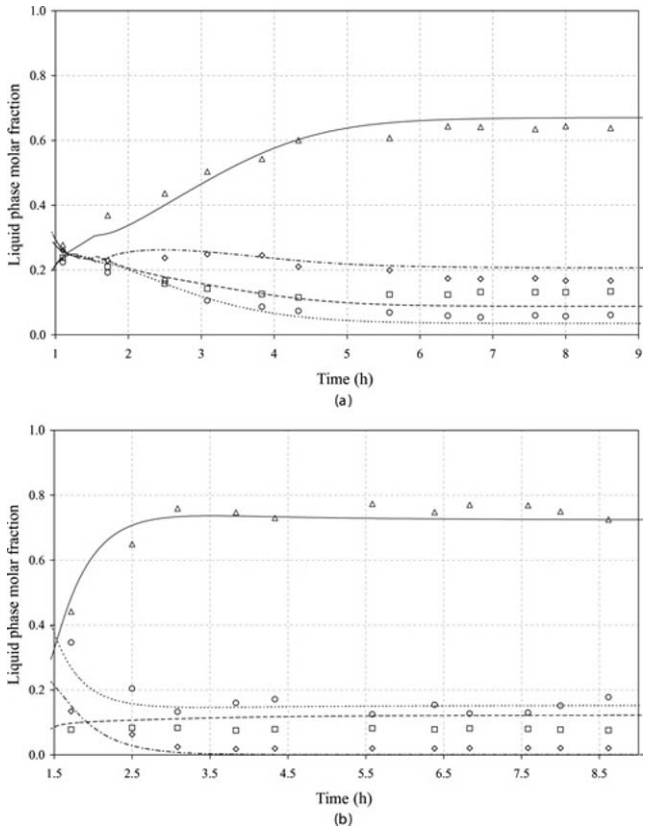

Figure 5. Dynamic composition trend in the reboiler (top) and of the organic phase in the decanter (bottom) from experiment and simulation. HOAc (▽,–dash-dot line–), PrOH (□, dashed line), PrOAc (Δ, solid line), H_2O (o, dotted line).

decanter, the reflux is turned on as soon as the first vapour condenses, otherwise (case 0) the decanter is first filled with the condensate. As in the experiments the organic phase is completely returned to the column as the reflux, the aqueous phase is withdrawn from the system. Specifications are taken from the experimental setup.

Figure 6 shows the comparison of the trends of the MX function (calculated for the organic phase in the decanter)

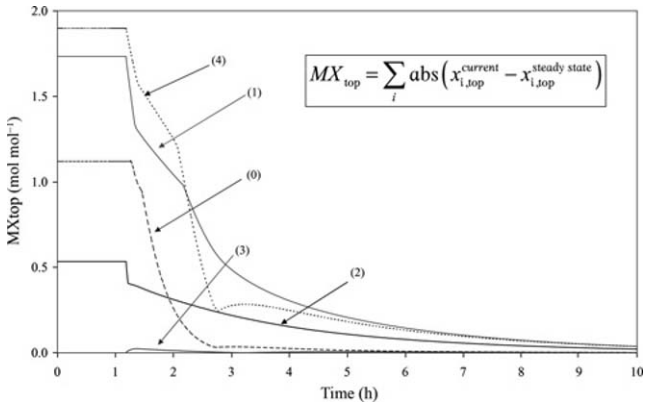

Figure 6. Comparison of the MXtop-function in the organic phase in the decanter during startup for different simulation runs. (0): initially empty decanter, (1): initial charging of *n*-propanol, (2): initial charging of *n*-propyl acetate, (3): initial charging with two phase mixture (steady state composition), (4): initial charging of acetic acid.

which gives the deviation of the current from the steady state composition for the different startup strategies. The strong influence of the composition of the initial charging can be seen. As expected, initial charging of the two-phase top product leads to the fastest startup (case 3) and reduces startup time compared to an initially empty decanter (case 0). The composition of the organic phase deviates only very little and only for a short period of time from the steady-state values. All other initial charging results in a slower startup. The prolonging of startup time due to charging of the two phase product to the decanter as described by Tran (2005) could therefore not be observed for this process.

Conceptual Design

The conceptual design of a high-purity *n*-propyl acetate production process is initiated on the basis of the method developed by Tang *et al.* (2005) assuming that any acetic acid esterification reactive distillation process includes both rectifying and stripping sections: for *n*-propyl acetate system, when most of acetic acid is consumed in the reactive section, composition at the top of the column is close to the minimum boiling ternary azeotrope located inside the two liquid phases region (Figure 7); thus a decanter is placed to remove the aqueous phase of the distillate whereas organic phase is further processed in a stripping column to obtain high-purity *n*-propyl acetate: Figure 8 regroups all studied flowsheets for this esterification.

The process design has been developed using a sequential approach based on steady-state simulations. The feasible values of different parameters leading to a PrOAc molar purity of 98% for each configuration [except (e) for which water content in product stream is remaining slightly higher than 2%)] are related in Table 5. The qualitative analysis of all possible flowsheets gives the following conclusions:

- the optimal feed tray for the acetic acid (high boiling reactant) is the column base unlike the usual double-feed configuration (the low-boiling reactant is fed in the reboiler and

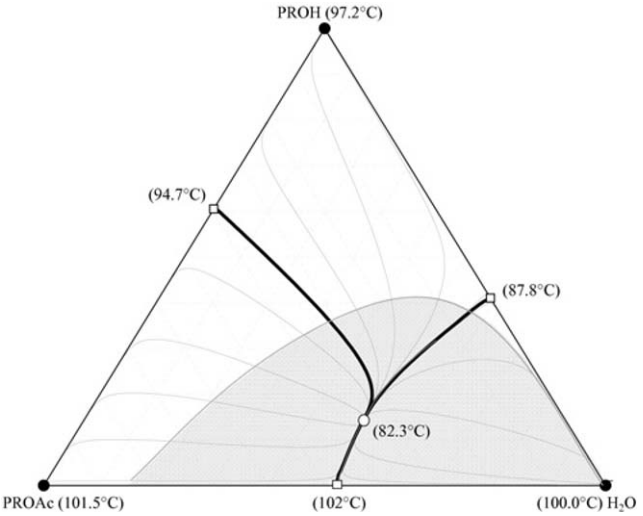

Figure 7. RCM of the PrOH/PrOAc/H_2O non-reactive mixture showing the miscibility gap, the distillation boundaries, the unstable (○) and stable nodes (•) and the saddle points (□).

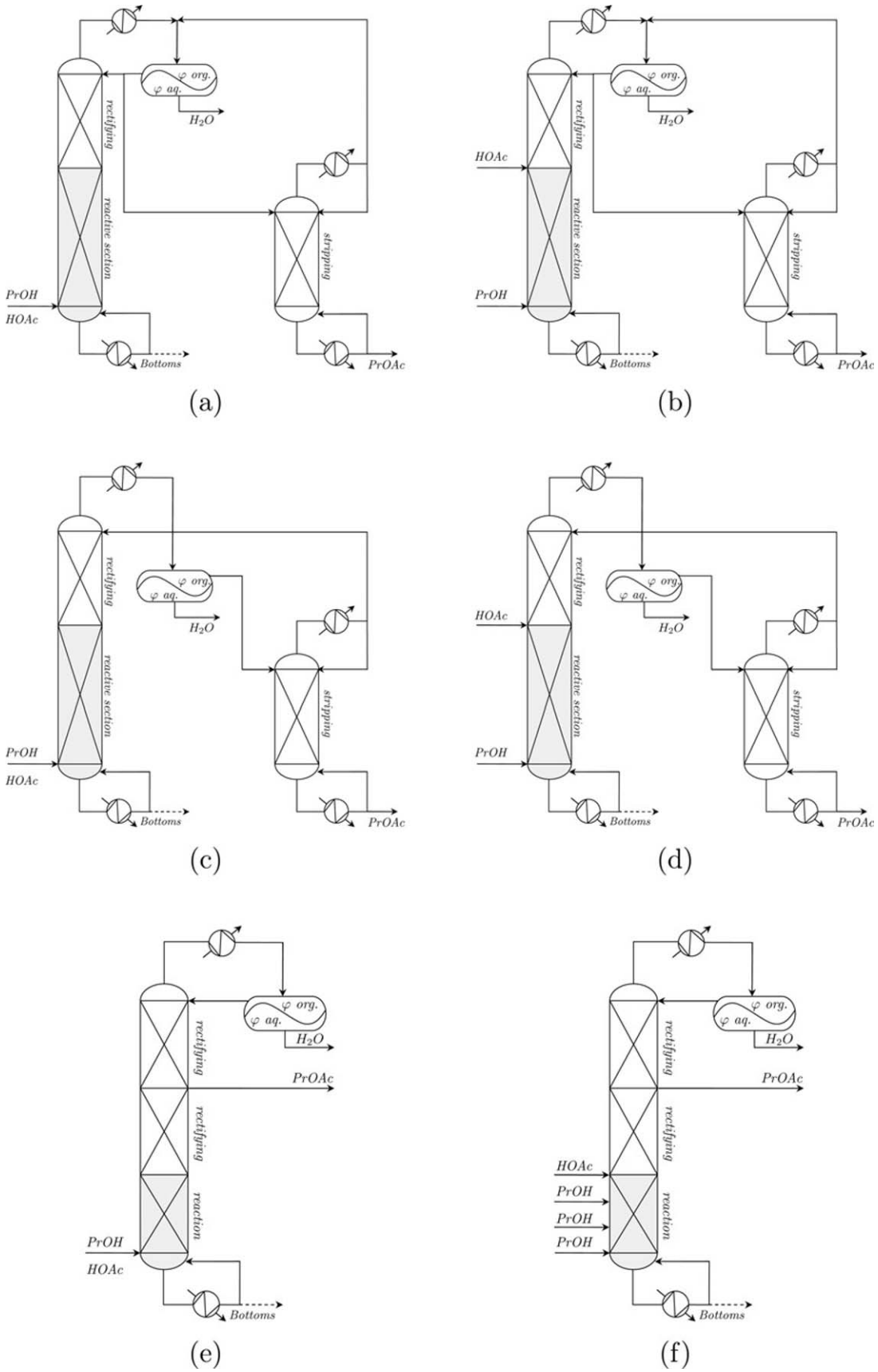

Figure 8. Six possible flowsheets for the *n*-propyl acetate production by catalytic reactive distillation (single/multiple feeds). (a) & (b) Partial withdrawal of the decanter organic phase towards an additional stripping column; (c) & (d) total withdrawal of the decanter organic phase towards an additional stripping column; (e) & (f) total reflux of the decanter organic phase in a single reactive distillation column with an intermediate PrOAc withdrawal.

Table 5. Feasible setups of the three single-feed configurations.

	(a)	(c)	(e)	(c')
Design variables				
NTS reactive section	15	15	16	15
NTS rectifying section	15	15	10 + 10	15
NTS stripping section	15	10	—	20
Operating variables				
F_{HOAc} (mol h^{-1})	83.26	83.26	83.26	83.26
F_{PrOH} (mol h^{-1})	84.03	84.03	84.03	84.03
Decanter temperature (°C)	20	20	20	20
Decanter reflux ratio[b]	0.923	0	∞	0
RD reboiler duty (kW)	4.468	5.025	6.220	6.205
Stripper reboiler duty (kW)	1.819	1.115	—	2.000
Stripper reflux ratio	4.985	1.000	—	1.000
Products				
PrOAc flow rate (mol h^{-1})	82.82	83.22	84.61	82.83
x_{HOAc}	0.0018	0.0003	0.0002	0.0005
x_{PrOH}	0.0182	0.0197	0.0023	0.0005
x_{PrOAc}	0.9800	0.9800	0.9770	0.9990
x_{H_2O}	0.0000	0.0000	0.0202	0.0000
H_2O flow rate (mol h^{-1})	82.24	82.11	82.33	84.22
x_{HOAc}	0.0004	0.0001	0.0000	0.0000
x_{PrOH}	0.0055	0.0023	0.0099	0.0109
x_{PrOAc}	0.0029	0.0015	0.0031	0.0032
x_{H_2O}	0.9912	0.9961	0.9870	0.9859
Bottoms flow rate (mol h^{-1})	2.22	1.97	0.35	0.24
x_{HOAc}	0.6551	0.6937	0.7402	0.7397
x_{PrOH}	0.1918	0.1702	0.1463	0.1466
x_{PrOAc}	0.1084	0.0972	0.0816	0.0817
x_{H_2O}	0.0447	0.0389	0.0319	0.0320
Molar conversion (%)	98.0	98.3	99.7	99.7
Recovery rate (%)	99.4	99.6	99.7	99.7
Performance index[b] (%)	97.4	98.0	99.3	99.4

[a]Ratio of the organic stream refluxed in the RD column on the withdrawn stream sent to the stripper.
[b]Ratio of molar PrOAc production on molar HOAc feed.

high-boiling above the reactive section); this can be explained since the reboiler holdup is larger than the column holdup;

- the bottom products may not always be neglected since depending on PrOAc stream specifications (purity and recovery rate), unreacted HOAc has to be withdrawn;
- a configuration with total withdrawal of the decanter organic phase [(c) and (d)] is more suitable to produce high-purity PrOAc; the last column in Table 5(c') shows that a quasi-pure PrOAc stream can be produced when the stripper NTS and the reboiler duties are increased;

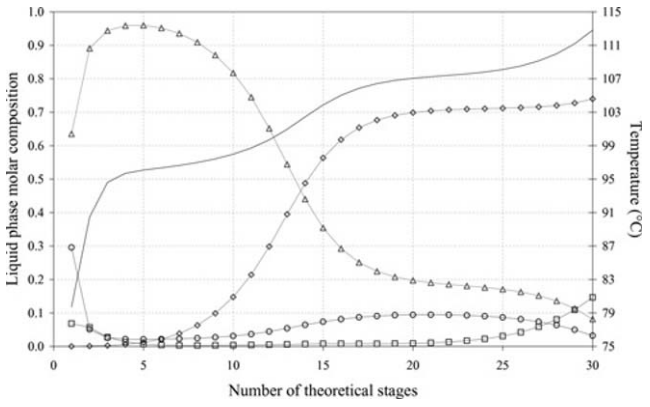

Figure 9. Liquid phase composition profiles and temperature along reactive distillation for type (c) process (PrOAc purity of 99.9%). HOAc (▽), PrOH (□), PrOAc (△), H_2O (○) and temperature (solid line).

- the single-column configuration with an intermediate PrOAc withdrawal (e) is powerful in terms of conversion and recovery, but seems not to be adapted to pure PrOAc production: water is still remaining in the product stream (2%) which may not be suitable. Moreover, an addition of 10 stages in the rectifying section results in only a slight improvement of PrOAc purity ($<0.1\%$).

Note that the number of theoretical stages in the rectifying section, the reflux ratio of organic phase of the decanter and the feed ratio are the main sensitive parameters. The rectifying section is required to decrease the acetic acid amount in the distillate (see liquid composition profiles Figure 9), but its concentration in the bottom products depends on the reaction conversion only: that's why a small alcohol excess is set in the feed. Some attempts of fractionating the alcohol feed were carried out in order to increase reaction rate on the upper stages of the reactive section, but no significant effect was found.

CONCLUSIONS

This study is focused on the conceptual design of high-purity *n*-propyl acetate production by reactive distillation. The first part of this article is devoted to experimental results obtained on two kinds of device: stirred reactor and RD pilot plant. A kinetic model for both homogeneously and heterogeneously catalysed reaction has been developed and chemical equilibrium data have been successfully compared with previous publications. The second part deals with the

simulation of the reactive distillation pilot plant. Model validation has been carried out with steady-state and dynamic data and an optimal startup strategy has been recommended using dynamic simulations. On this basis, six different setups have been identified as being able to product high-purity *n*-propyl acetate; a single-feed configuration with a decanter at the top of the column and the further purification of all the decanter organic withdrawal has been noticed to be the most suitable design to achieve such a production.

In the near future, an optimal design of a catalytic distillation column will be achieved based on our model and using MINLP approach; finally, the performances of this new design will be experimentally checked in an heterogeneous catalysed column located in TU Berlin.

NOMENCLATURE

a	liquid phase activity
Δn	molar transformation, mol
E	energy of activation, J mol^{-1}
F	flow rate, mol h^{-1}
K	equilibrium constant
K_o	preexponential factor
HU	hold-up, mol
n	molar amount, mol
p	pressure, bar
Q	reboiler duty, kW
r	rate of reaction, mol s^{-1}
T	temperature, K
v	molar volume, m^3/ mol
V	volume, m^3
x	liquid phase composition

Subscripts and superscripts

a	activity
f	forward (esterification)
i	component index
j	stage index
L	liquid
LV	boiling point
o	reference or initial state
V	vapour

REFERENCES

Bart, H.J., Kaltenbrunner, W. and Landschutzer, H., 1996, Kinetics of esterification of acetic acid with propyl alcohol by heterogeneous catalysis, *Int J Chem Kinetics*, 28: 649–656.

Brehelin, M., Rouzineau, D., Thery, R., Meyer, X. and Meyer, M., 2006, Calcul des courbes de résidu réactif hétérogène de la reaction de synthèse de l'acétate de *n*-propyle, *Proceedings of SIMO'06*.

Chiang, S.F., Kuo, C.L., Yu, C.C. and Wong, D.S.H., 2002, Design alternatives for the amyl acetate process—coupled reactor column and reactive distillation, *Ind Eng Chem Res*, 41: 3233–3246.

Engel, V., Stichlmair, J. and Geipel, W., 2001, Fluid dynamics of packings for gas-liquid contactors, *Chem Eng Technol*, 24(5): 459–462.

Fillon, M., Meyer, M., Pingaud, H. and Joulia X., 1995, Data reconciliation based on elemental balances applied to batch experiments, *Comput Chem Eng*, 19S: 293–299.

Huang, Y.S., Sundmacher, K., Tulashie, S. and Schlünder, E.U., 2005, Theoretical and experimental study on residue curve maps of propyl acetate synthesis reaction, *Chem Eng Sci*, 60: 3363–3371.

Marek, J.and Standart, G., 1954, Vapor–liquid equilibria in mixtures containing an associating substance. II. Binary mixtures of acetic acid at athmospheric pressure, *Collect Czech Chem Comm*, 19: 1074–1084.

Okasinski, M.J. and Doherty, M.F., 2000, Prediction of heterogenenous reactive azeotropes in esterification systems, *Chem Eng Sci*, 55: 5263–5271.

Pitochelli, A.R., 1980, Ion exchange catalysis and matrix effects (Rhom and Haas Co., Philadelphia, PA).

Reepmeyer, F., Repke, J.-U. and Wozny, G., 2004, Time optimal start-up strategies for reactive distillation columns, *Chem Eng Sci*, 59(20): 4339–4347.

Sørensen, J.M. and Arlt, W., 1982, *Liquid-Liquid Equilibrium Data Collection. Chemistry Data Series*, (Dechema).

Steinigeweg, S., 2003, *Zur Entwicklung von Reaktivrektifikationsprozessen am Beispiel gleichgewichtslimitierter Reaktionen* (Shaker Verlag Aachen Germany).

Steinigeweg, S. and Gmehling, J., 2002, *n*-Butyl acetate synthesis via reactive distillation thermodynamic aspects, reaction kinetics, pilot-plant experiments, and simulation studies, *Ind Eng Chem Res* 41:, 5483–5490.

Tang, Y.T., Chen, Y.W., Huang, H.P., Yu, C.C., Hung, S.B. and Lee, M.J., 2005, Design of reactive distillation for acetic acid esterification, *AIChE J*, 51(6): 1683–1699.

Tran, T.K., 2005, *Analyse des Anfahrens von Dreiphasenkolonnen* (Shaker Verlag, Aachen, Germany).

Ung, S. and Doherty, M.F., 1995, Vapor–liquid phase equilibrium in systems with multiple chemical reactions, *Chem Eng Sci*, 50: 23–48.

Weisz, P.B. and Hicks, J.S., 1962, The behaviour of porous catalyst particles in view of internal mass and heat diffusion effects, *Chem Eng Sci*, 17: 265–275.